Fusion Engineering and Design 222 (2026) 115403

Contents lists available at ScienceDirect

Fusion Engineering and Design

journal homepage: www.elsevier.com/locate/fusengdes

Feasibility study of gamma-ray spectroscopy for the determination of the fusion power at the SPARC tokamak☆

Simone Lorenzo Fugazza [a], Giulia Marcer [b], Massimo Nocente [a,*], Alessandro Ciurlino [a], Gabriele Croci [a], Marco Dalla Rosa [a], Andrea Dal Molin [a], Erik Gallo [c], Giuseppe Gorini [a,b], Miriam Parisi [c], Prasoon Raj [d], Marica Rebai [b], Matthew Reinke [d], Davide Rigamonti [b], Federico Scioscioli [a,b], Marco Tardocchi [b], JET Contributors[1]

[a] Department of Physics - University of Milano Bicocca, Piazza della Scienza 3, Milan, 20126, Italy
[b] Institute for Plasma Science and Technology - National Research Council, Via Roberto Cozzi 53, Milan, 20125, Italy
[c] Eni S.p.A., Piazzale Enrico Mattei 1, Rome, 00144, Italy
[d] Commonwealth Fusion Systems, 117 Hospital Rd, Devens, 01434, MA, USA

ARTICLE INFO

Keywords:
Nuclear fusion
Tokamak
Gamma ray
Neutron
Diagnostics
SPARC
Fusion power

ABSTRACT

SPARC is a high-field, compact tokamak aiming to obtain a fusion gain Q>1 in Deuterium-Tritium (DT) plasmas for the first time in a magnetic confinement fusion reactor. Fusion power measurement is a key diagnostic requirement. In this work we present a scoping study of a gamma-ray spectrometer for the determination of the fusion power at SPARC. Measurements are based on the detection of the 16.7 MeV and ~ 14 MeV gamma-rays produced by the weak secondary channel $T(D,\gamma)^5He$ of the DT fusion reaction, whose branching ratio has been recently measured at the JET tokamak. Starting from the numerical calculation of the DT gamma source and a first evaluation of the sources of background radiation, we determine the fusion power range where measurements are possible at SPARC. We find that the fusion power can be determined in the broad range of 0.2 MW to 140 MW, when different neutron and gamma-ray attenuators are employed depending on the operational conditions. Potential additional applications of the gamma-ray detector scoped in this work are also briefly discussed.

1. Introduction

One of the primary objectives of nuclear fusion research is achieving a fusion gain Q > 1 in Deuterium-Tritium (DT) plasmas. This means that the fusion power produced exceeds the input power required to keep the plasma sufficiently hot. Tokamaks like ITER and SPARC must achieve this milestone to advance nuclear fusion commercialization.

A key factor in calculating Q is measuring the fusion power. In DT plasmas, absolute measurements of neutron yield are obtained using flux monitors cross-calibrated with activation foils. Although this method is well-established, it comes with challenges: significant MonteCarlo (MC) modelling of the machine is necessary, followed by extensive in-situ calibration campaigns. These procedures need to be repeated whenever modifications to the machine vessel are made [1].

An alternative method to measure the fusion power can leverage on measurements of the gamma-rays produced by the weak secondary channel $T(D,\gamma)^5He$ of the DT fusion reaction. When this occurs, the ^5He nucleus born from D+T fusion, rather than splitting into a neutron and an alpha particle, decays either to its ground or first excited state, leading to the emission of a gamma-ray with average energy 16.75 MeV (γ_0) or ~14 MeV (γ_1), respectively [2]. The feasibility of the method in a tokamak environment has been recently proven in DT experiments at the JET tokamak [3], where a value of $(2.4 \pm 0.5) \cdot 10^{-5}$ γ/n has been determined for the branching ratio of the de-excitation of the ^5He nucleus by gamma-ray emission with respect to the more common disintegration in a neutron and an alpha particle [4].

Although complicated by the need to handle the significant neutron and gamma-ray background that is produced together with the γ_0 and γ_1 emissions, one main advantage of the method is that it relies on modelling of gamma-ray (rather than neutron) transport in the tokamak, which is a comparatively much simpler task. Moreover, even in machines where the determination of the fusion power by neutron

☆ This article is part of a Special issue entitled: 'SOFT 2024' published in Fusion Engineering and Design.

* Corresponding author.
E-mail address: massimo.nocente@unimib.it (M. Nocente).

[1] See the author list of "C.F. Maggi et al 2024 Nucl. Fusion 64 112012 https://doi.org/10.1088/1741-4326/ad3e16"

https://doi.org/10.1016/j.fusengdes.2025.115403
Received 27 November 2024; Received in revised form 27 June 2025; Accepted 23 August 2025
Available online 12 September 2025
0920-3796/© 2025 The Authors. Published by Elsevier B.V. This is an open access article under the CC BY license (http://creativecommons.org/licenses/by/4.0/).

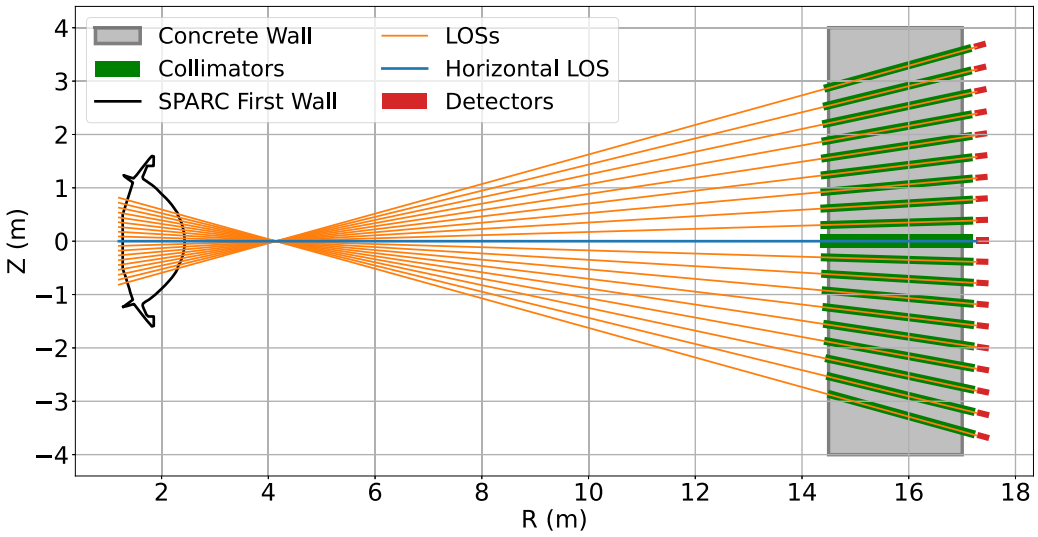

Fig. 1. A schematic of the SPARC neutron camera. A 2.4 m thick wall separates the Diagnostic Hall from the Tokamak Hall. 19 lines of sight (labelled "LOSs" in the figure) observe the plasma from a radial field of view. R and Z are the radial and vertical cylindrical coordinates, respectively, with the origin at the torus centre.

measurements remains the main method, measurements of the γ_0 and γ_1 emission are still valuable as an independent way to validate fusion power measurements by neutron diagnostics.

Building on the recent experimental progress described above, in this paper we present the scoping study of a gamma-ray detector designed for fusion power measurements at SPARC. SPARC is a compact ($R_0 = 1.85$ m) and high magnetic field ($B_0 \sim 12$ T) tokamak [5] currently being developed by Commonwealth Fusion Systems (CFS) which aims to demonstrate DT plasmas with Q > 1 for the first time in a tokamak.

The paper is organized as it follows. After the detector specification provided in Section 2, we describe the numerical evaluation of the signal and background sources in Section 3. The results are used to identify the fusion power range where measurements are feasible, depending on the set of neutron and gamma-ray attenuators that is used. We finally discuss the limitations of our method and briefly mention some other diagnostic applications [6] that the detector could contribute to, leaving their detailed exploration to future work.

2. A gamma ray detector for SPARC

We base our scoping study on the $LaBr_3$:Ce scintillator spectrometer, as this has been successfully used for the DT gamma measurements at the JET tokamak [7,8], and adopt the same dimensions (a cylinder of 3″ × 6″, diameter × length). The detector still represents the state of the art for gamma-ray spectroscopy in fusion plasmas, thanks to its short decay time (30 ns), enabling gamma-ray measurements at MHz counting rates [9,10], high photon yield (61/keV) [11], and energy resolution (3.8% at 662 keV) [12,13].

The SPARC facility will have a dedicated area for nuclear diagnostics, referred to as the Diagnostic Hall. This will be separated from the Tokamak Hall by a thick concrete wall, approximately 2.4 m thick. A Neutron CAMera (NCAM) with up to 19 channels is being designed, providing a set of radial views in the poloidal cross section. The separation distance between adjacent channels is about 40 cm at the detectors position ($R \gtrsim 17.0$ m, from the centre of the SPARC torus) and about 7 cm inside the plasma ($R = 1.85$ m).

In this scoping study, we assume that the gamma diagnostic can be placed along one of the NCAM lines of sight, at a distance $R > 17$ m. For example, the gamma diagnostics could be integrated with one of the planned NCAM spectrometers for neutron measurements along the NCAM channels, by placing the diagnostics behind the diamond detector. In this study we assume that collimators with a diameter $D = 1$ cm are expected for all channels, except for the central one, which has a diameter $D = 3$ cm [14]. Indeed, to compensate for the low efficiency of the magnetic proton recoil spectrometer planned for the central channel, a wider collimator is employed to ensure a sufficiently high neutron flux. Fig. 1 shows a schematic view of the NCAM.

3. Fusion power measurements at SPARC

3.1. Signal evaluation

To determine whether gamma-based fusion power measurements will be feasible in SPARC, we must first estimate the DT-gamma signal counting rate at the detector. We require that the fusion power is measured with at least 10% accuracy over a time scale of 1 s. Considering the Poisson statical nature of the measurement, this implies a minimum counting rate at the detector of 100 Hz. For comparison, a statistical accuracy of 1% would correspond to a counting rate of 10 kHz at the detector, which may be desired to counteract additional systematic uncertainties that may affect the measurement (see later).

In order to assess the feasibility of the measurement, we have evaluated the counting rate expected when the detector is positioned at the end of each channel of the NCAM. This was done by using the REVOLT [15] MC code for the numerical description of each line of sight in combination with GENESIS [16] for the evaluation of the neutron and gamma-ray radiation source due to the fusion reactions. Based on the geometrical input parameters for each line of sight, REVOLT determines the plasma region seen by the detector, dividing it into smaller volume pixels (voxels). For each voxel, the code evaluates the emission direction that the radiation must have to reach the detector, as well as the transport factor, which is proportional to the fraction of solid angle where the radiation must be emitted to reach the detector.

The evaluation of the DT-gamma emissivity source has been made with GENESIS, which makes use of the line of sight information provided by REVOLT to evaluate the radiation intensity (gamma/second) that reaches the front surface of the detector. Input parameters for GENESIS are the SPARC magnetic equilibrium (flux surfaces) and plasma profiles (temperature and density). It is further assumed that the fuel ions are in local thermal equilibrium, so that their distribution functions are described by a Maxwellian. In our calculations we have used magnetic and kinetic profiles for the Q = 11 scenario (corresponding to an expected fusion power of 140 MW) available in the paper [17]

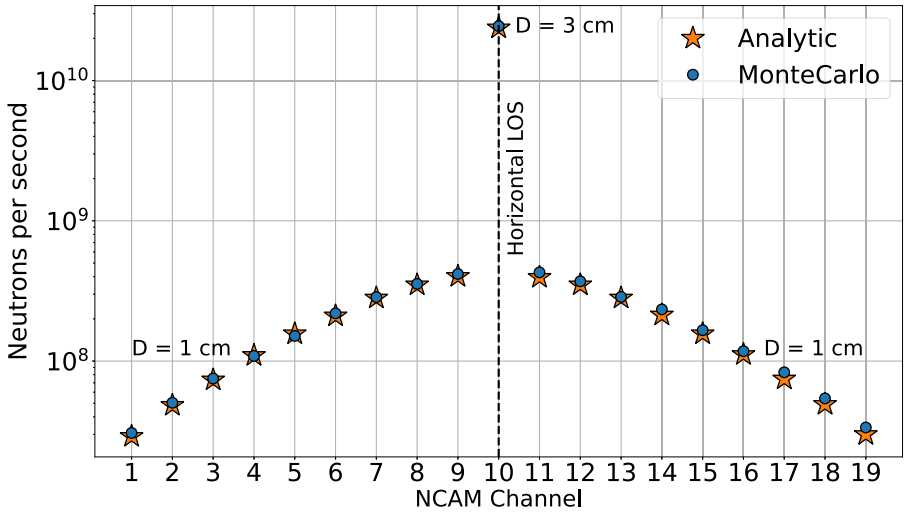

Fig. 2. MC (GENESIS+REVOLT) and semi-analytical results (Lynalitic) of the expected DT direct neutron rate for each detector in the NCAM. Notice that the highest rates are observed along the central horizontal channel (Channel #10), which views the plasma core and is equipped with a larger collimator. Channels from #1 to #19 have a collimator diameter D = 1 cm, except for Channel #10 with D = 3 cm.

Table 1
DT neutrons and gammas per second at the detector front surface calculated via GENESIS for SPARC NCAM Channel #9 (D = 1 cm) and #10 (D = 3 cm).

NCAM channel	DT-Neutrons (Hz)	DT-Gammas (Hz)
Channel#9	4.2 10^{8}	1.0 10^{4}
Channel#10	2.4 10^{10}	5.8 10^{5}

and in the SPARC GitHub open repository [18]. Signals for lower fusion power scenarios are obtained from those corresponding to 140 MW by linear down scaling.

Fig. 2 shows results on the neutron signal (neutron/s) expected at the front surface of each channel of the NCAM. Note that, primarily as a result of the collimator size, the intensity of the signal along the central channel (3 cm diameter) is rather different from that along all the others (1 cm diameter). As expressed in the following equation, adapted from [19]:

$$r_{n,\gamma} = \epsilon_{n,\gamma} \frac{\pi}{64} \left(\frac{d_D \, d_C}{L} \right)^2 \int_{\lambda} y_{n,\gamma}(s) \, ds \tag{1}$$

the neutron and gamma-ray rates are proportional to the square of both the detector diameter (d_D) and the collimator diameter (d_C). When the two diameters are approximately equal ($d = d_C \approx d_D$), the resulting signal scales as $\propto d^4$. The other terms in Eq. (1) include: $\epsilon_{n,\gamma}$, the full-energy peak efficiency of the detector; L, the length of the collimator; λ, the line of sight (assuming a narrow field of view); and $y(s)$, the neutron or gamma-ray emissivity along λ.

The corresponding gamma-ray signal is obtained by multiplying the neutron signal with the branching ratio and is reported in Table 1 for the most central channels.

The numerical calculations based on coupling GENESIS and REVOLT (indicated by circles in Fig. 2) have been bench-marked by independent semi-analytical calculations (stars). These have been based on the Linalytic code, as described in [20]. Linalytic, unlike GENESIS and REVOLT, combines analytical and numerical methods to calculate the transport factors. The two methods agree within 5% for the most peripheral channels and better than 1% for the central channel, which provides confidence on the validity of the calculations of the signal, particularly for the central channels.

3.2. Background sources

We now address the background sources that affect fusion power measurements using gamma spectrometry. One source comes from the direct neutrons produced by the main fusion reaction and which will reach the detector with the intensities shown in Fig. 2 and Table 1 if no dedicated neutron attenuator is used. Another source is due to prompt gamma-rays born from the interaction between the direct neutrons and the tokamak structures. This turns out to be the main limiting factor for fusion power measurements using gamma spectrometry, but it can be addressed by the use of dedicated gamma-ray attenuators of different length, determined depending on the operational range.

3.2.1. Direct neutron background

The $LaBr_3$:Ce detector is highly sensitive (efficiency ~1) to neutrons [21,22] implying that, without neutron attenuators, the detector would experience counting rates well in excess of 10 MHz. For comparison, fusion power measurements at the JET tokamak were shown to be possible for total counting rates <500 kHz [4], with pile-up and detector stability being the main limiting factors above this experimental counting rate threshold.

To counteract the background contribution from direct neutrons, we have to include a neutron attenuator in the SPARC detector application. Based on the experience at JET and successful tests at nuclear accelerators [23,24], this is a cylindrical sample of LiH with 1.2 m length and a diameter that matches that of the $LaBr_3$:Ce scintillator. Based on previous calculations [19], which have been recently benchmarked by measurements at JET, 1.2 m of LiH can attenuate 14.1 MeV neutrons by a factor of 10^6 and the high energy gamma-rays of interest for fusion power measurements by a factor 8 only.

Table 2 lists the neutron and gamma-ray intensities that may be observed at Channels #9 and #10 of the NCAM with and without the 1.2 m LiH attenuator for the Q = 11 scenario. We find that the intensity due to direct neutrons would always lead to a counting rate well in excess of 500 kHz if no LiH attenuator is used. Acceptable measurement conditions (statistical uncertainty in the range 1% to 10%) can be achieved both on channel #9 and #10 (central), although statistical uncertainties better than 1% can be achieved using channel #10 only. However, we here stress that these considerations do not take into account additional sources of background, such as that arising from prompt gamma-rays, as discussed in the next section. As far as the background contribution of scattered neutrons is concerned, based on the JET measurements this can be reduced to a few % by a well collimated line of sight, such as that designed for the SPARC NCAM, and it is therefore neglected in this scoping study.

Table 2
Intensities at the detector front surface for direct DT neutrons and DT gamma-rays with and without 1.2 m of LiH, calculated along Channels #9 and #10. In the "Comment" columns, intensities are marked as "Not acceptable" when in excess of 500 kHz; "Desired" when they lead to a statistical uncertainty better than 1%; "Acceptable" when leading to an uncertainty between 1% and 10%.

DT-Particle and attenuator	Intensities (Hz) at Ch#9	Comment (Ch#9)	Intensities (Hz) at Ch#10	Comment (Ch#10)
Neutron (no LiH)	4.2 10^{8}	Not acceptable	2.4 10^{10}	Not acceptable
Gamma (no LiH)	1.0 10^{4}	Desired	5.8 10^{5}	Not acceptable
Neutron + LiH	4.2 10^{2}	Acceptable	2.4 10^{4}	Acceptable
Gamma + LiH	1.0 10^{3}	Acceptable	5.8 10^{4}	Desired

3.2.2. Neutron-induced prompt gamma-ray background

Another important source of background comes from the prompt gamma-rays that originate from the interaction of neutrons with the tokamak structures, as observed at JET. The origin of this further contribution is due to the fact that the footprint of the line of sight intercepts the machine inboard first wall and the vacuum vessel. These structures are constantly impacted by the intense neutron emission from the plasma, leading to the production of prompt gamma-rays, with a fraction of them reaching the detector through the line of sight, as also verified by comprehensive MCNP [25] simulations for the JET case [26,27]. In absence of detailed Monte Carlo models of SPARC, we have developed an empirical method to estimate the prompt gamma-ray background at SPARC based on the JET data, as described below.

Assuming a known neutron flux F_n^{in} on the tokamak first wall, the outgoing F_γ^{out} prompt gamma-ray flux can be expressed as the product of a prompt gamma-ray emission probability P and F_n^{in}, i.e.

$$P = F_\gamma^{out} / F_n^{in} \tag{2}$$

Unlike F_γ^{out}, as fusion neutrons are all born with an energy of 14 MeV irrespective of the device, we surmise that P is independent of the intensity of the neutron source, but may have a dependence on the material composition of the tokamak structures.

For the JET case, we can use the data collected in fusion power measurement experiments by the Tangential Gamma Ray Spectrometer (TGRS) [7,20,28] diagnostic to evaluate P. The TGRS system [28] consists of a 3" × 6" $LaBr_3$:Ce detector with a LiH attenuator, characterized by a line of sight tangential to the inner wall and lying on the JET equatorial plane. The $LaBr_3$:Ce detector observes two sections of the wall (one at the inner and one at the outer wall) while passing twice through the plasma core.

From the JET experience with TGRS, we can establish that the majority of the gamma ray background is concentrated below 10 MeV. This fact suggests that, while prompt gamma-rays constitute an important radiation load for the detector, they interfere little within the spectral region associated with the γ_0 and γ_1 signals. If we interpret all the events in the spectral region below 10 MeV as primarily due to prompt gamma-rays, also considering that direct and scattered neutrons are almost fully suppressed by the use of LiH for the TGRS, we can estimate the gamma-ray flux at the locations of the first wall that are intersected by the line of sight, assuming only geometrical transport through the line of sight. This, combined with the evaluation of the neutron flux on the first wall from the known total neutron emission, leads to a prompt gamma-ray emission probability P.

The value of P was recently estimated from the analysis of 96 discharges of the DTE2 campaign at JET, resulting in $P = 4.7\%$ [20].

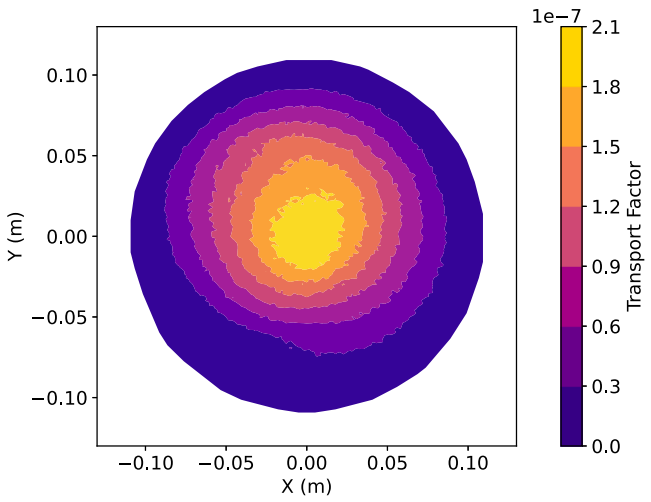

Fig. 3. Contour plot of the SPARC wall section observed frontally by the detector along the Channel #10 horizontal line of sight. The brightness corresponds to the transport factor of each pixel.

3.3. Gamma-ray spectrometer operational range

To determine the operational range for fusion power measurement using gamma spectrometry at SPARC, we must now evaluate the background that will be present together with the signal of Fig. 2. To do this, we assume that the detector is placed at a distance of 1.3 m behind the central channel of the NCAM to allow for some space that may be needed in an actual implementation of the diagnostics. Similar results in terms of fusion power operational range are obtained if the detector is placed right behind the central channel, although the background due to prompt gamma-ray emission is found to be roughly 2 times larger in such case. In order to evaluate the contribution of prompt gamma-rays to the background at the detector, we have used REVOLT to model the transport factors of the prompt gamma-rays emitted by the area of the first wall that is intercepted by the detector line of sight, with the results shown in Fig. 3.

The prompt gamma-ray source to which the transport factors of Fig. 3 are applied has been evaluated by multiplying the neutron flux on the first wall for the Q > 11 scenario of SPARC with the probability P obtained from the JET data. While P may be different in SPARC with respect to JET (and cannot currently be evaluated as we lack both a MCNP model and experimental data for SPARC) only an increase of P by more than an order of magnitude, which we deem unlikely, would eliminate the scope for fusion power measurements at SPARC. Calculation of background fluxes due to prompt gamma-rays have been made for all channels and added to those from the direct neutrons. The final result on the operational range for fusion power measurements is shown for channel #10 in Fig. 4. In this figure, the two horizontal lines represent the practical requirements for good measurements based on the JET experience, namely that the signal leads to a counting rate of at least 100 Hz and that the overall counting rate on the detector (signal+background) is below 500 kHz. The oblique lines show the expected signal and background level for different fusion power levels where, as noted above, calculations have been made using the kinetic and magnetic equilibrium profiles of the Q > 11 scenario and linearly down-scaled for lower fusion power levels. We find that, without additional gamma-ray attenuators, there is a fusion power window of about 1.8 orders of magnitudes, between 0.2 MW and up to 13.2 MW, where measurements are possible. We also note that, once the LiH neutron attenuator is in place, the prompt gamma-ray background becomes the main factor that sets the upper bound of the window for fusion power measurements by gamma-ray spectroscopy. For channels

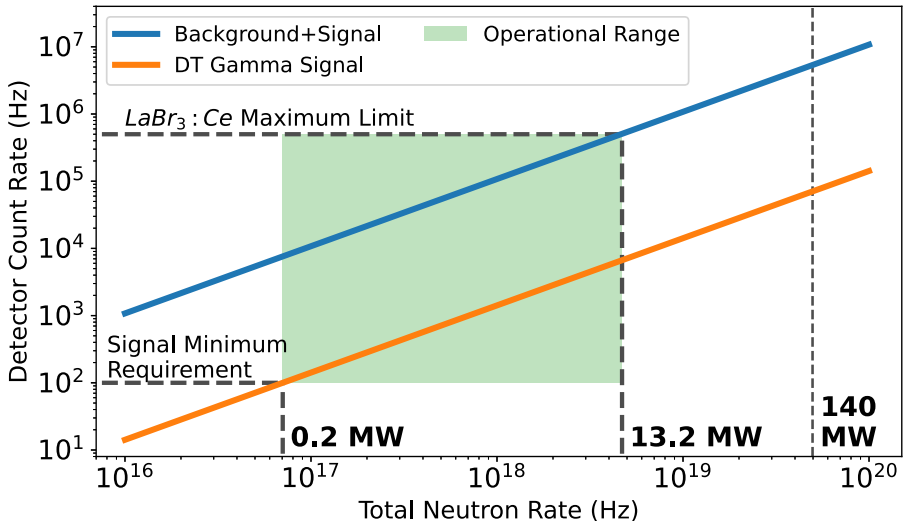

Fig. 4. Expected count rate at the $LaBr_3$:Ce detector (with a LiH attenuator) when placed along Channel #10 of the SPARC-NCAM. The horizontal lines indicate the practical requirements for good measurements, namely that the signal counting rate is at least 100 Hz and the overall counting rate does not exceed 500 kHz. The operational range for fusion power measurements is indicated by the green shaded area.

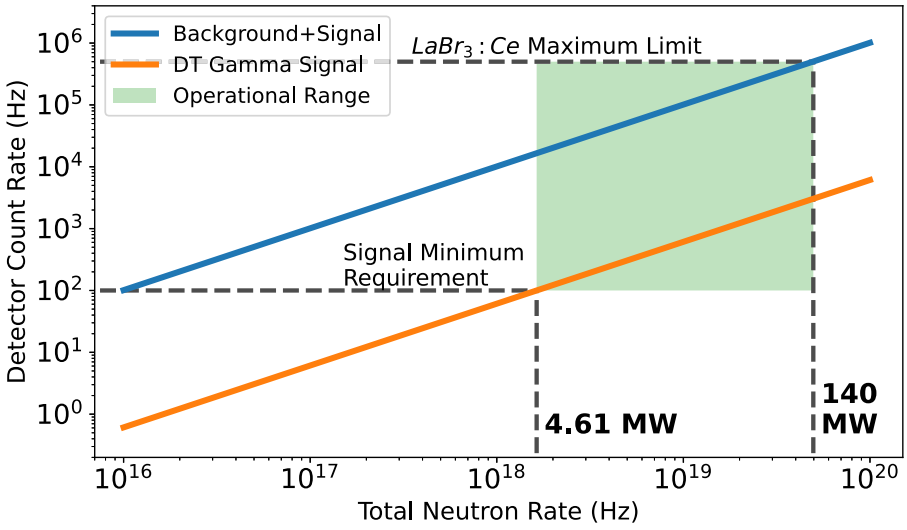

Fig. 5. Expected count rate at the $LaBr_3$:Ce detector (with a LiH neutron attenuator and a 3.0 cm tungsten attenuator) when placed along Channel #10 of the SPARC-NCAM. The horizontal lines indicate the practical requirements for good measurements, namely that the signal counting rate is at least 100 Hz and the overall counting rate does not exceed 500 kHz. The operational range for fusion power measurements is indicated by the green shaded area.

other than #10, due to their smaller diameter of 1 cm in the currently assumed NCAM design, the window for fusion power measurements has an extent that is less than a factor 2, which makes these channels impractical for this application.

While the results of Fig. 4 suggest that there is a relatively large window where fusion power measurements are possible at SPARC, provided that a sufficiently large collimator and a LiH neutron attenuator are used, it would be desirable to find ways to centre the fusion power measurement window at higher powers. This is possible by adding gamma-ray attenuators to the setup, such as tungsten.

Based on the Lambert–Beer law, the gamma-ray intensity $I(x)$, after travelling a distance x, is attenuated according to

$$I(x) = I_0 \exp(-\mu x) \tag{3}$$

where I_0 is the initial intensity and μ is an attenuation coefficient depending on both the material and the gamma ray energy. We have used the NIST database [29] to find the length l required for the tungsten attenuator to enable an upper boundary of 140 MW for the fusion power range, leading to $l = 3.0$ cm.

Fig. 5 illustrates the operational range of the $LaBr_3$:Ce detector for SPARC when a 3.0 cm tungsten attenuator is added to the 1.2 m LiH neutron attenuator. There is now a new measurement range that extends from ~5 MW up to the maximum projected fusion power, 140 MW. We note that, in the 140 MW scenario, DT-gamma count rates of about 3.04 kHz are expected, corresponding to a statistical uncertainty of 1.8%.

4. Discussion

The calculations presented in this paper suggest that there is scope for the development of a gamma-ray spectrometer for fusion power measurements at the SPARC tokamak. Their accuracy level is however not yet sufficient to proceed towards the actual development of the detector, as our findings are subject to some assumptions and limitations, which are discussed here.

One main limitation comes from the evaluation of the prompt gamma-ray background at SPARC. For this contribution, as described

in Section 3.2.2, we have used JET data to infer the emission probability P and used that for SPARC. As the exact value of P depends on the mix of materials used for the SPARC tokamak, which may be different than those of JET, it is likely that our evaluation of P comes with some systematic uncertainty, perhaps of a factor 2 or 3. The uncertainty on P for SPARC ultimately impacts the extent of the operational range where fusion power measurements are possible (see Fig. 5). For example, if P were larger by a factor of 2, the operational range would correspondingly be reduced by the same factor. However, as Figs. 4 and 5 show, fusion power measurements at SPARC seem to be possible over more than an order of magnitude. This suggests that the operational window would be null only if P were larger by more than a factor 10 than assumed here, which we deem unlikely. More generally, there is a need to better understand the neutron-induced reactions that lead to the background observed for the measurements at JET, for example by attempting to reproduce the observed spectral shape and intensity of the background using an MC model. In this way, materials that contribute the most to the background could be identified and a more detailed evaluation of the background at SPARC could be made, which is required to enable the actual development of the gamma-ray detector. Ultimately, the accurate evaluation of the background at SPARC would have to rely on an MCNP model, once sufficient knowledge on the most relevant processes that affected the background in the measurements at JET is gained.

Other aspects that require further study towards the development of an actual detector for SPARC are the neutron and gamma-ray attenuators. Concerning neutrons, our study has been based on the use of LiH, which has been tested at JET. However, there are some safety concerns which make LiH not ideal for use in a high performance tokamak. LiH is a hazardous material which undergoes violent exothermic reactions with water, even in the form of moist air. Additionally, even if properly sealed, it can release hydrogen at high temperature, leading to detonation. For this reason, we are presently seeking alternative attenuators that provide a similar, excellent neutron abatement factor, but pose less challenging safety hazards and are thus easier to integrate in a tokamak such as SPARC.

Concerning the gamma-ray attenuator, our evaluations have been based on the use of tungsten, as it can be easily manufactured and is widely available. The gamma-ray attenuation of tungsten is however higher for the signal ($I_0/I(l) \approx 23$ at the energies corresponding γ_0 and γ_1 emissions) than the background, which has an average energy of 4 MeV ($I_0/I(l) \approx 11$ at this energy). This is the reason why the operational window of Fig. 5 is reduced by about 2.5 with respect to that of Fig. 4. Ideally, one would like to find a gamma-ray attenuator that has a larger abatement factor at the gamma-ray energies of the background, which may be possible by studying the attenuation properties of other high Z materials than tungsten.

We further note that this study does not consider other factors that require a detailed evaluation for the actual development of the diagnostics, such as the detailed (i.e. not just geometrical) transport of both the signal and background gamma rays through ports and collimators.

The main motivation of this work has been to scope a gamma-ray spectrometer for fusion power measurements at SPARC, as this is a key parameter for a machine than aims at reliably producing plasmas with $Q > 1$ up to $Q > 11$. We however note that the same instrument could contribute to a broader range of physics studies, as demonstrated at JET [6]. Examples are the diagnostics of ions accelerated to the MeV range by radio-frequency [30,31], for example ^{3}He and protons in the planned hydrogen and ^{3}He minority scenarios [17,32], or the diagnostics of the runaway electron energies during the startup of the discharge or in dedicated experiments [10,33]. A highly desired capability for a gamma-ray detector in DT plasmas is the diagnostics of the fusion born alpha particles. Unlike JET, where alpha particle diagnostics by gamma-ray spectroscopy have been relying on reactions between the alpha particles and ^{9}Be impurities naturally present in the plasma due to the beryllium first wall, in SPARC, where the first wall will primarily be made of tungsten [32,34], different reactions would have to be relied on. A possibility could be to exploit the $^{10}\mathrm{B}(\alpha, \mathrm{p}\,\gamma)^{13}\mathrm{C}$ reaction [35], which leads to the generation of gamma-rays at the energies 3.09, 3.68 and 3.85 MeV. The boron impurities required for the reaction could either be injected on purpose using pellets, or could be available in the plasma as a legacy of the conditioning of the first wall using boron ("boronization") [36,37]. Unlike reactions with beryllium, the cross sections of $^{10}\mathrm{B}(\alpha, \mathrm{p}\,\gamma)^{13}\mathrm{C}$ are however not as well measured and there is currently no experimental demonstration on the use of such reactions to measure properties of the alpha particles. For example, the minimum amount of boron impurities required to measure a statistically meaningful signal is not known, as well as the overall spectral shape due to the combination of the three emission lines at 3.09, 3.68 and 3.85 MeV, convolved with the instrument response function. While we are currently performing first studies to establish the experimental basis for alpha particle measurements via the $^{10}\mathrm{B}(\alpha, \mathrm{p}\,\gamma)^{13}\mathrm{C}$ reaction in SPARC and elsewhere, we anticipate that the prompt gamma-ray background analysed in Section 3.2.2 will be a limiting factor. Such background may even have a more severe impact for this application, as the $^{10}\mathrm{B}(\alpha, \mathrm{p}\,\gamma)^{13}\mathrm{C}$ signal falls in the same spectral region of the background, which requires a careful evaluation.

5. Conclusion

A scoping study of a gamma ray detector to determine the fusion power at the SPARC tokamak has been made. Measurements are based on the detection of the 16.7 MeV and ≈14 MeV gamma-rays produced by the weak secondary channel $\mathrm{T(D,\gamma)^5He}$ of the DT fusion reaction, whose branching ratio has been recently measured at the JET tokamak. Based on the numerical calculation of the DT gamma source, and an estimation of the sources of background radiation due to neutrons and prompt gamma-rays, we find that there is an operational window of more than an order of magnitude where the fusion power can be determined, in the range of 0.2 MW to 13.2 MW if a 1.2 m LiH is used as the neutron attenuator, without gamma-ray attenuators. By the addition of tungsten attenuators with a variable length up to 3.0 cm, measurements over the full operational range 0.2 MW to 140 MW are deemed possible with a statistical accuracy of at least 10%, when the fusion power is provided every second. The background due to the emission of prompt gamma-rays that enter the line of sight and are due to neutrons interacting with the tokamak structures is identified as the main limiting factor for the measurement and needs to be better evaluated. Besides fusion power measurements, the detector could serve additional scopes, such as the diagnostics of runaway electrons, fast ions generated by radio-frequency heating or alpha particles born from the fusion reactions, which will be the subject of future studies.

CRediT authorship contribution statement

Simone Lorenzo Fugazza: Writing – review & editing, Writing – original draft, Visualization, Validation, Software, Formal analysis, Conceptualization. **Giulia Marcer:** Writing – review & editing, Visualization, Validation, Software, Formal analysis, Conceptualization. **Massimo Nocente:** Writing – review & editing, Writing – original draft, Visualization, Supervision, Methodology, Conceptualization. **Alessandro Ciurlino:** Formal analysis. **Gabriele Croci:** Conceptualization. **Marco Dalla Rosa:** Formal analysis. **Andrea Dal Molin:** Conceptualization. **Erik Gallo:** Funding acquisition, Conceptualization. **Giuseppe Gorini:** Supervision, Conceptualization. **Miriam Parisi:** Funding acquisition, Conceptualization. **Prasoon Raj:** Conceptualization. **Marica Rebai:** Conceptualization. **Matthew Reinke:** Conceptualization. **Davide Rigamonti:** Conceptualization. **Federico Scioscioli:** Conceptualization. **Marco Tardocchi:** Supervision, Project administration, Conceptualization.

Declaration of competing interest

The authors declare the following financial interests/personal relationships which may be considered as potential competing interests: Simone Lorenzo Fugazza reports financial support was provided by Eni SpA Marco Dalla Rosa reports financial support was provided by Eni SpA. If there are other authors, they declare that they have no known competing financial interests or personal relationships that could have appeared to influence the work reported in this paper.

Acknowledgements

This research was made possible through the support of Commonwealth Fusion Systems, USA and the funding provided by Eni SpA, Italy, which also supports the PhD scholarships of Simone Lorenzo Fugazza and Marco Dalla Rosa, Italy.

This work has been carried out within the framework of the EUROfusion Consortium, funded by the European Union via the Euratom Research and Training Programme (Grant Agreement No 101052200 - EUROfusion). Views and opinions expressed are however those of the author(s) only and do not necessarily reflect those of the European Union or the European Commission. Neither the European Union nor the European Commission can be held responsible for them.

Data availability

Data will be made available on request.

References

[1] D.B. Syme, et al., Fusion yield measurements on JET and their calibration, in: Nuclear Engineering and Design, Selected and Expanded Papers from International Conference Nuclear Energy for New Europe 2010, Portorož, Slovenia, September 6-9, 2010, vol. 246, (ISSN: 0029-5493) 2012, pp. 185–190, http://dx.doi.org/10.1016/j.nucengdes.2011.08.003.

[2] F. Ajzenberg-Selove, Energy levels of light nuclei A = 5–10, Nucl. Phys. A (ISSN: 0375-9474) 490 (1) (1988) 1–225, http://dx.doi.org/10.1016/0375-9474(88)90124-8.

[3] M. Rebai, et al., First direct measurement of the spectrum emitted by the ^{3}H(^{2}H, γ)^{5}He reaction and assessment of the relative yield γ_1 to γ_0, Phys. Rev. C 110 (1) (2024) 014625, http://dx.doi.org/10.1103/PhysRevC.110.014625, Publisher: American Physical Society.

[4] A. Dal Molin, et al., Measurement of the Gamma-Ray-to-Neutron branching ratio for the Deuterium-Tritium Reaction in magnetic confinement fusion plasmas, Phys. Rev. Lett. 133 (5) (2024) 055102, http://dx.doi.org/10.1103/PhysRevLett.133.055102, Publisher: American Physical Society.

[5] A.J. Creely, et al., Overview of the SPARC tokamak, J. Plasma Phys. 86 (5) (2020) 865860502, http://dx.doi.org/10.1017/S0022377820001257, ISSN: (1469) 0022-3778-7807.

[6] M. Nocente, et al., MeV range particle physics studies in tokamak plasmas using gamma-ray spectroscopy, Plasma Phys. Control. Fusion (ISSN: 0741-3335) 62 (1) (2019) 014015, http://dx.doi.org/10.1088/1361-6587/ab4f32, Publisher: IOP Publishing.

[7] M. Nocente, et al., A new tangential gamma-ray spectrometer for fast ion measurements in deuterium and deuterium–tritium plasmas of the joint european torus, Rev. Sci. Instrum. 92 (4) (2021).

[8] M. Nocente, et al., Fusion product measurements by nuclear diagnostics in the joint european torus deuterium–tritium 2 campaign, Rev. Sci. Instrum. 93 (9) (2022).

[9] M. Nocente, et al., High resolution gamma ray spectroscopy at MHz counting rates with $LaBr_3$ scintillators for fusion plasma applications, IEEE Trans. Nucl. Sci. 60 (2) (2013) 1408–1415.

[10] M. Nocente, et al., High resolution gamma-ray spectrometer with MHz capabilities for runaway electron studies at asdex upgrade, Rev. Sci. Instrum. 89 (10) (2018).

[11] E.V.D. van Loef, et al., Scintillation properties of $LaBr_3$:Ce3+ crystals: Fast, efficient and high energy-resolution scintillators, Nucl. Instrum. Methods Phys. Res. Sect. A: Accel. Spectrometers Detect. Assoc. Equip. (ISSN: 0168-9002) 486 (1) (2002) 254–258, http://dx.doi.org/10.1016/S0168-9002(02)00712-X, Proceedings of the 6th International Conference on Inorganic Scintillators and their Use in Scientific and Industrial Applications.

[12] M. Nocente, et al., Energy resolution of gamma-ray spectroscopy of JET plasmas with a $LaBr_3$ scintillator detector and digital data acquisition, Rev. Sci. Instrum. (ISSN: 0034-6748) 81 (10) (2010) 10D321, http://dx.doi.org/10.1063/1.3501386.

[13] D. Rigamonti, et al., The upgraded JET gamma-ray cameras based on high resolution/high count rate compact spectrometers, Rev. Sci. Instrum. (ISSN: 0034-6748) 89 (10) (2018) 10I116, http://dx.doi.org/10.1063/1.5038839.

[14] P. Raj, et al., Overview of the neutron diagnostic systems for the SPARC tokamak, Rev. Sci. Instrum. (ISSN: 0034-6748) 95 (10) (2024) 103507, http://dx.doi.org/10.1063/5.0219538.

[15] A. Celora, et al., A multipurpose numerical method for imaging studies and tomographic reconstruction, J. Inst. 19 (03) (2024) C03032, http://dx.doi.org/10.1088/1748-0221/19/03/C03032.

[16] M. Nocente, Neutron and Gamma-Ray Emission Spectroscopy As Fast Ion Diagnostics in Fusion Plasmas (Ph.D. dissertation), University of Milano-Bicocca, 2012, Available: https://boa.unimib.it/handle/10281/28397.

[17] P. Rodriguez-Fernandez, et al., Predictions of core plasma performance for the SPARC tokamak, J. Plasma Phys. 86 (5) (2020) 865860503, http://dx.doi.org/10.1017/S0022377820001075, ISSN: (1469) 0022-3778-7807.

[18] Cfs-energy/SPARCPublic, 2022, [Online]. Available: https://github.com/cfs-energy/SPARCPublic. (Accessed 16 October 2024).

[19] M. Nocente, et al., Conceptual design of the radial gamma ray spectrometers system for α particle and runaway electron measurements at ITER, Nucl. Fusion (ISSN: 0029-5515) 57 (7) (2017) 076016, http://dx.doi.org/10.1088/1741-4326/aa6f7d, Publisher: IOP Publishing.

[20] G. Marcer, A Novel Method for DT Fusion Power Measurement in Magnetic Confinement Plasmas Based on the Gamma Ray Emission from the D(T, ^{5}He)γ Reaction, University of Milano-Bicocca, 2025, Available: https://boa.unimib.it/handle/10281/543003.

[21] C. Cazzaniga, et al., Response of LaBr3(Ce) scintillators to 14 MeV fusion neutrons, Nucl. Instrum. Methods Phys. Res. Sect. A: Accel. Spectrometers Detect. Assoc. Equip. (ISSN: 0168-9002) 778 (2015) 20–25, http://dx.doi.org/10.1016/j.nima.2015.01.002.

[22] C. Cazzaniga, et al., Response of LaBr3(Ce) scintillators to 2.5 MeV fusion neutrons, Rev. Sci. Instrum. (ISSN: 0034-6748) 84 (12) (2013) 123505, http://dx.doi.org/10.1063/1.4847056.

[23] I.N. Chugunov, et al., Testing the neutron attenuator based on ^{6}LiH for γ-ray diagnostics of plasmas in the JET tokamak, Instrum. Exp. Tech. (ISSN: 1608-3180) 51 (2) (2008) 166–170, http://dx.doi.org/10.1134/S0020441208020024.

[24] D. Rigamonti, et al., Role of neutron attenuators for gamma-ray measurements in deuterium–tritium magnetic confinement plasmas, Rev. Sci. Instrum. (ISSN: 0034-6748) 93 (9) (2022) 093515, http://dx.doi.org/10.1063/5.0101783.

[25] Monte carlo n-particle, Online. Available: https://mcnp.lanl.gov/.

[26] A. Zohar, et al., Validation of realistic Monte Carlo plasma gamma-ray source on JET discharges, Nucl. Fusion (ISSN: 0029-5515) 62 (6) (2022) 066004, http://dx.doi.org/10.1088/1741-4326/ac50c0, Publisher: IOP Publishing.

[27] A. Zohar, et al., Modelling of plasma gamma ray sources in large tokamaks, Fusion Eng. Des. (ISSN: 0920-3796) 163 (2021) 112158, http://dx.doi.org/10.1016/j.fusengdes.2020.112158.

[28] G. Marcer, et al., Study of a single line of sight gamma ray diagnostics for measurements of the absolute gamma ray emission from JET, J. Instrum. (ISSN: 1748-0221) 16 (12) (2021) 012019, http://dx.doi.org/10.1088/1748-0221/16/12/C12019.

[29] X-Ray Mass Attenuation Coefficients, NIST, 2009, [Online]. Available: https://www.nist.gov/pml/x-ray-mass-attenuation-coefficients. (Last Modified: 2022-02-17T15:37-05:00).

[30] M. Nocente, et al., High-resolution gamma ray spectroscopy measurements of the fast ion energy distribution in JET 4 He plasmas, Nucl. Fusion (ISSN: 0029-5515) 52 (6) (2012) 063009, http://dx.doi.org/10.1088/0029-5515/52/6/063009, Publisher: IOP Publishing and International Atomic Energy Agency.

[31] M. Nocente, et al., Generation and observation of fast deuterium ions and fusion-born alpha particles in jet plasmas with the 3-ion radio-frequency heating scenario, Nucl. Fusion 60 (12) (2020) 124006.

[32] P. Rodriguez-Fernandez, et al., Overview of the SPARC physics basis towards the exploration of burning-plasma regimes in high-field, compact tokamaks, Nucl. Fusion (ISSN: 0029-5515) 62 (4) (2022) 042003, http://dx.doi.org/10.1088/1741-4326/ac1654, Publisher: IOP Publishing.

[33] A. Shevelev, et al., Study of runaway electron dynamics at the asdex upgrade tokamak during impurity injection using fast hard x-ray spectrometry, Nucl. Fusion 61 (11) (2021) 116024.

[34] T. Gray, et al., Divertor Component Testing, Tech. Rep. ORNL/SPR–2022/2536, 1993696, NFE-20-08060, 2022, http://dx.doi.org/10.2172/1993696, ORNL/SPR–2022/2536, 1993696, NFE–20–08 060.

[35] V. Kiptily, et al., Escaping alpha-particle monitor for burning plasmas, Nucl. Fusion 58 (8) (2018) 082009, http://dx.doi.org/10.1088/1741-4326/aab676, ISSN: (1741) 0029-5515-4326.

[36] G.L. Jackson, et al., Boronization in DIII-d, J. Nucl. Mater. Plasma-Surface Interact. Control. Fusion Devices (ISSN: 0022-3115) 196–198 (1992) 236–240, http://dx.doi.org/10.1016/S0022-3115(06)80038-3.

[37] U. Schneider, et al., Boronization of ASDEX, J. Nucl. Mater. (ISSN: 0022-3115) 176–177 (1990) 350–356, http://dx.doi.org/10.1016/0022-3115(90)90071-T.